Vol 17 No 6, June 2008
1674-1056/2008/17(06)/2130-07

Chinese Physics B

© 2008 Chin. Phys. Soc.
and IOP Publishing Ltd

Micro thermal shear stress sensor based on vacuum anodic bonding and bulk-micromachining*

Yi Liang(易 亮)[a)b)], Ou Yi(欧 毅)[a)†], Shi Sha-Li(石莎莉)[a)‡],
Ma Jin(马 瑾)[b)], Chen Da-Peng(陈大鹏)[a)], and Ye Tian-Chun(叶甜春)[a)]

[a)] *Silicon Device & Integrated Technology Department, Institute of Microelectronics of Chinese Academy of Sciences, Beijing 100029, China*

[b)] *School of Physics & Microelectronics, Shandong University, Jinan 250100, China*

(Received 8 September 2007; revised manuscript received 17 October 2007)

This paper describes a micro thermal shear stress sensor with a cavity underneath, based on vacuum anodic bonding and bulk micromachined technology. A Ti/Pt alloy strip, 2μm×100μm, is deposited on the top of a thin silicon nitride diaphragm and functioned as the thermal sensor element. By using vacuum anodic bonding and bulk-si anisotropic wet etching process instead of the sacrificial-layer technique, a cavity, functioned as the adiabatic vacuum chamber, 200μm×200μm×400μm, is placed between the silicon nitride diaphragm and glass (Corning 7740). This method totally avoid adhesion problem which is a major issue of the sacrificial-layer technique.

Keywords: thermal micro shear stress sensor, vacuum anodic bonding, bulk-micromachined
PACC: 4000, 4700, 4715c, 4200

1. Introduction

The measurement of wall shear stress is very important in fluid mechanics and aerodynamics studies. It can be used in control of flow separation in the design of high-performance aircraft. For example, Jiang *et al*[1−3] worked on a new way of controlling an Unmanned Aerial Vehicle (UAV) through the sensing/controlling of the flow separation on the curved leading edge of the wing. This requires distributed shear-stress sensors mounted on the curved surface of the leading edge to measure the shear-stress profile.

Techniques for measuring the shear stress can be categorized into indirect and direct methods.[4,5] Direct measurement relies on the detection of the total amount of viscous drag experienced by a surface-mounted force balance. The drag force represents the area integration of the shear force. In order to obtain high sensitivity, it is desirable to have large surface areas in order to increase the amount of drag force and induced displacement. In indirect methods, the shear stress is extracted from other measured physical parameters (e.g., pressure and wall temperature) which are related to the shear stress. However, ports for pressure measurements require modification to the wall and present potential disturbance to the flow. Flow measurement based on thermal transfer principles is an indirect method and has been widely used.[4] Examples include flow-rate sensors with hot-wire or hot-film configurations. In comparison with pressure measurement techniques, thermal sensors can be used in a wide variety of flow conditions and present minimal disturbance to the flow itself because of the surface flush mount. Huang *et al*[6] compared the performances of micro thermal shear stress sensors with and without cavity underneath. They found that the former has a higher sensitivity than the latter. The cavity significantly decreased the heat loss to the substrate.

It is well known that the cavity under the micro thermal shear stress sensor is difficultly formed by sacrificial layer technology, for the thin diaphragm above the cavity tends to adhere to the substrate when etching and releasing the sacrificial layer. Common avoiding adhesion method such as using bumps formed by dry etching and chemical vapour deposition (CVD) of the sacrificial layer is not applicable for the case of mi-

*Project supported by the National Natural Science Foundation of China (Grant No 60576053) and Technology Innovation of Chinese Academy of Sciences (Grant No CXJJ-176).
†Corresponding author. E-mail: ouyi@ime.ac.cn
‡Corresponding author. E-mail: shishali@ime.ac.cn

cro thermal shear stress sensor. This method is based on vacuum anodic bonding and bulk-si anisotropic wet etching process instead of sacrificial-layer technique.

This paper describes a micro thermal shear stress sensor with a cavity underneath, based on vacuum anodic bonding and bulk micromachined technology. This method, which makes the process very easy, not only avoids adhesion problem, but also does not influence the vacuum chamber's adiabatic effect. Such presented novel micro thermal shear stress sensor can be designed and fabricated by MEMS fabrication technique.

2. Principles

The principles of micro thermal shear stress sensor[7,8] are briefly described below. The sensor consists of a thermal sensor element located on the surface of a diaphragm. The thermal sensor element resides with a velocity boundary layer in which the velocity changes from zero (at the wall) to the value of the mean-stress flow. The shear stress is expressed as:

$$\tau_{\mathrm{w}} = \mu \frac{\mathrm{d}U_y}{\mathrm{d}y}. \tag{1}$$

Where μ is the viscosity of the fluid and U_y is the flow velocity at a distance y from the wall. As a result, the flow shear stress determines the rate of heat transfer from the heated element to the surrounding flow field.

The temperature change of the resistor can be measured by the change in its resistance. The resistance R of a semiconductor sensing element at an elevated temperature T is expressed as

$$R = R_0[1 + \alpha(T - T_0)]. \tag{2}$$

Where R_0 is the resistance at the room temperature T_0, α is the temperature coefficient of resistance often termed TCR.

A thermal boundary layer is characterized as a region where temperature gradients are presented in the flow. Typical profiles of thermal and velocity boundary layers are illustrated in Fig.1 for the case of a two-dimensional (2D) heat generating/sensing element inside of a 2D channel flow. Within the thermal boundary layer, flow temperature decreases with increasing distance away from the heated element until the temperature reaches that of the mean stream flow.

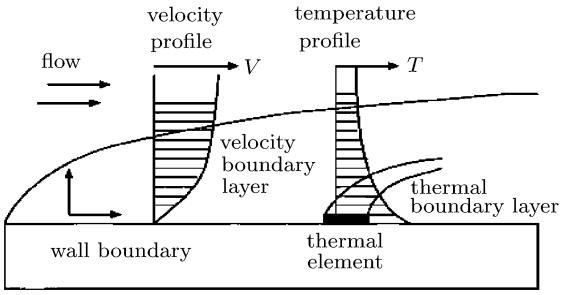


Fig.1. Velocity and temperature boundary layers.

The relationship between T_{w} and the temperature of the heated resistor has been studied[9] under a major assumption that the thermal boundary layer of the thermal element lies within the velocity boundary layer. Under several other assumptions, the relationship between the input power, shear stress at the wall, and temperature of the thermal element can be expressed in simply analytical form. These assumptions include: (1) the thermal transfer in the span-wise direction can be ignored and (2) effects of natural convection are much smaller in comparison with forced convection. Under ohmic heating, the input power is related to the driving current and the sensor resistance. Since part of the input power is transferred to the flow while the rest is lost through the substrate, the power balance is expressed as:

$$i^2 R = Q_{\mathrm{T}} + Q_{\mathrm{C}}. \tag{3}$$

Where Q_{T} represents the transferred convection heat to the flow, and Q_{C} represents the conduction heat loss to the substrate.

$$Q_{\mathrm{T}} = A(T - T_0)(\rho\tau_{\mathrm{w}})^{1/3}, \tag{4}$$

$$A = 0.8074 A_{\mathrm{e}} \left(\frac{C_{\mathrm{P}} K_{\mathrm{T}}}{L\mu} \right). \tag{5}$$

Here, A_{e} is the effective area of the thermal element, C_{P} is the heat capacity of the flow, K_{T} is the thermal conductivity of the fluid, L is the stream-wise length of the resistor, and μ is the viscosity.

At a certain input power i^2R, the greater the term Q_{C} is compared with $A\tau_{\mathrm{w}}^{1/3}$, the smaller the shear-stress sensitivity will be. Therefore, to design a successful thermal shear stress sensor, the heat loss to the substrate must be minimized.

3. Design and fabrication

Figure 2 shows the schematic top view of a thermal shear stress sensor and side view corresponding to the cross line on the top. The sensing element, $2\mu m \times 100\mu m$, $0.2\mu m$ thick, is located at the centre of a cavity diaphragm, which is typically $200\mu m \times 200\mu m$ in area and $1.5\mu m$ in thickness. Two metallization wires connect the resistor to the external electronics. The diaphragm is separated from the bottom of the cavity by proximately $400\mu m$ distance using the method of vacuum anodic bonding and bulk-si anisotropic wet etching technology. The pressure inside the cavity is about 0.05 Pa.

3.1. Structure design

3.1.1. Material selection

Ti/Pt alloy material is chosen as heating and sensing element. Silicon nitride is chosen as the diaphragm material, because it has low thermal conduction and can effectively prevent the thermal loss of heating element to the substrate. Glass (corning 7740) is chosen to anodic bonding with the substrate.

3.1.2. Structure design

The basic thermal shear stress sensor structure is that the diaphragm lies on the top of the vacuum cavity, with the glass sealed the bottom of the substrate. Vacuum cavity minimizes the heat conduction from the diaphragm to the substrate through the chamber, which offers effective thermal isolation between the heated element and the substrate. This anodic bonding chamber avoids using complicated sacrificial-layer technique. It is not only very easy to fabricate, but also does not influence the vacuum chamber's adiabatic effect. In addition, the sensor can be easily fabricated.

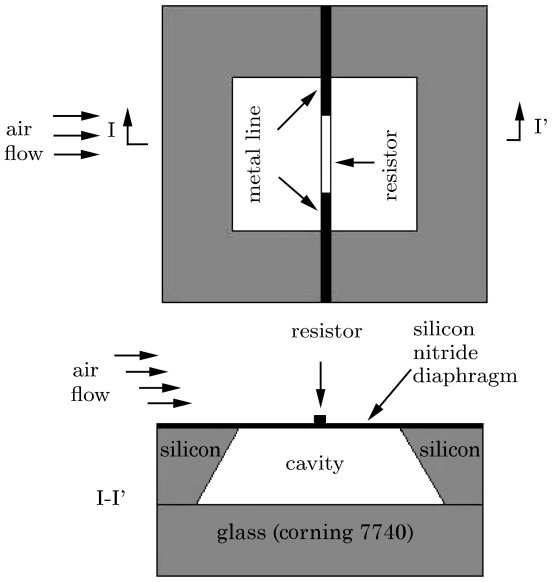


Fig.2. Schematic top and cross-sectional views (along line I-I') of a thermal shear stress sensor.

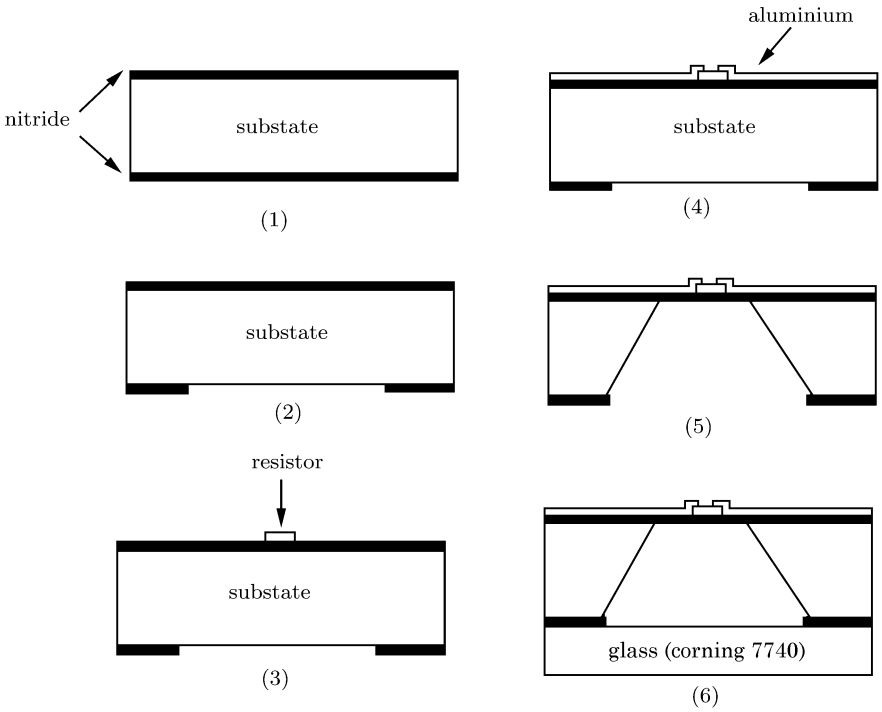


Fig.3. Main steps of the fabrication process of a shear-stress sensor.

3.2. Fabrication

The shear-stress sensors are fabricated with silicon bulk micro-machining technology. The process consists typically of three steps of photolithography—the etch window patterning, resistor definition and metallization patterning, as shown schematically in Fig.3. The first step is the deposition of a both-side low stress SiN_x film of thickness 1.5μm on a 2-in-diameter 0.4 mm thick silicon wafer (100), and then the backside is photo lithographically patterned to define the etching window in which the silicon nitride material is removed by using plasma etching to form a 900× 900μm^2 square window.

Second, the photolithography is done to pattern the resistor and then the Ti/Pt alloy resistor of 0.2μm thick is sputtered on the front side. After the lift-off, thermal evaporation produces the aluminium metallization (0.3μm) which is patterned to form the leads.

This is followed by bulk-si anisotropic wet etching on the backside which is in order to form the cavity. Before the etching process, the front side of the wafer is protected by crystal-bonding. Then, KOH (30%) solution anisotropic wet etching on the backside is performed and an air cavity that consists of four (111) plane of the silicon wafer is fabricated. A 200×200μm^2 windows is formed which is underneath the nitride diaphragm after etching.

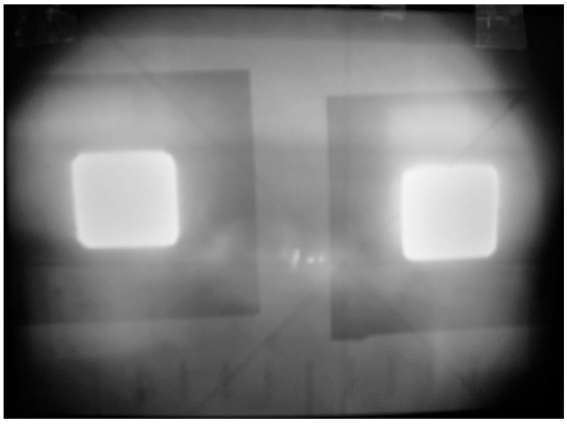


Fig.4. Infrared micrograph of a shear-stress sensor with a vacuum cavity.

Finally, the anodic bonding is done between the backside of the wafer and glass (Corning 7740) under vacuum environment (0.05 Pa). The voltage and the temperature is 1200V and 400°C respectively. Anodic bonding is probably the most versatile bonding process that can be used to permanently bond glass to silicon[10,11] and the cavity pressure can be successfully controlled once the anodic bonding is done successfully.

Figure 4 shows infrared micrograph of the fabricated devices we designed. The cavity is 200×200μm^2 on the top and 900×900μm^2 on the bottom.

4. Experimental results

4.1. Temperature coefficient of resistance

A hot plate is used to heat up the sensors and measure the resistance at different temperatures in order to measure the TCR. The measured data of a typical resistor is plotted in Fig.5. Adequate time delay is allowed between each temperature change to reach thermal equilibrium. To obtain TCR, we use the relation that $R = R_0(1 + \alpha(T - T_0))$ to fit the data where α is the TCR. A resistor has a typical positive TCR value of approximately 0.18%/°C.

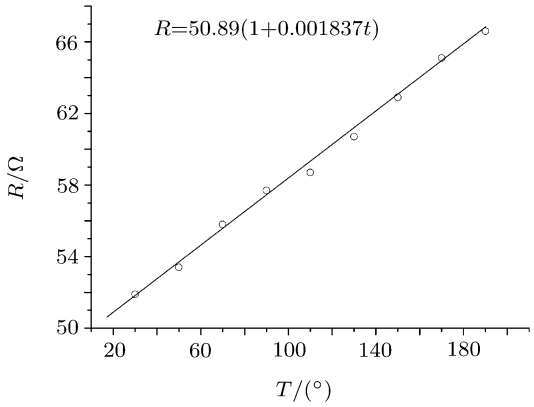


Fig.5. Resistance vs temperature measurement for a Ti/Pt alloy resistor on the silicon substrate.

4.2. Thermal isolation

The performance of the thermal isolation for our shear-stress sensors is evaluated next. Three sensor structures are prepared for obtaining current-voltage characteristics[7] (Fig.6). Diagram shows the first structure in which the resistor resides on top of a standard vacuum cavity. In the second structure, the anodic bonding between wafer and glass is not performed, thus, the cavity becomes filled with air, which will increase the thermal conduction between the thermal element and the substrate. In the last case, a reference sensor resistor, identical with the first two resistors in geometry and resistance, sit directly on

top of silicon substrate without cavity. Results of $I-V$ measurements conducted in still air are shown in Fig.7. It is clear that the resistor on the vacuum cavity has the largest non-linearity because the vacuum cavity offers the best thermal isolation. On the other hand, the $I-V$ curve of the resistor which directly resides on the silicon substrate is almost linear. This phenomenon indicates that the thermal conduction to the substrate dominates the heat transfer process and little temperature variation has been created.

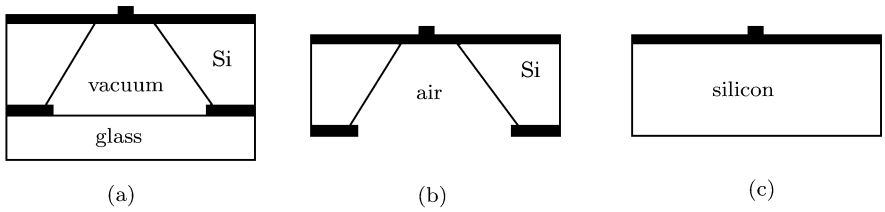


Fig.6. Schematic diagrams of (a) a Ti/Pt resistor located over a vacuum cavity, (b) on top of an air-filled cavity and (c) an identical resistor directly on top of the substrate.

Figure 8 shows the resistance as a function of power inputs by using the data from Fig.7. Furthermore,using the data form Fig.7 and the known TCR of the resistors, we can deduce the relationship between resistor temperature and power inputs as showed in Fig.9. It is found that the slope of the resistor over the vacuum cavity is 8×10^3°C/W,6.8×10^3°C/W for over the air-filled cavity, and 2×10^2°C/W for over the substrate. It is clear that a vacuum cavity improves the thermal isolation about 1.17 times over an air-filled cavity, and about 40 times over just the silicon substrate.

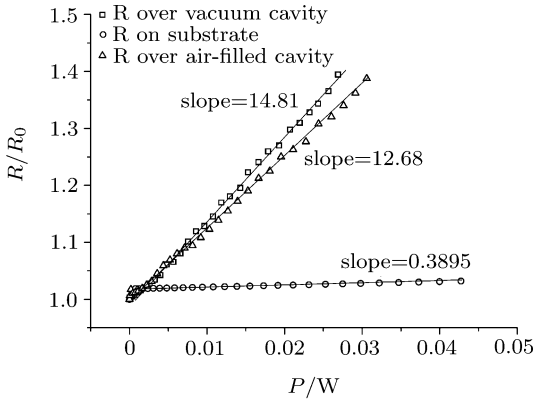


Fig.8. Calculated result of resistance vs power inputs.

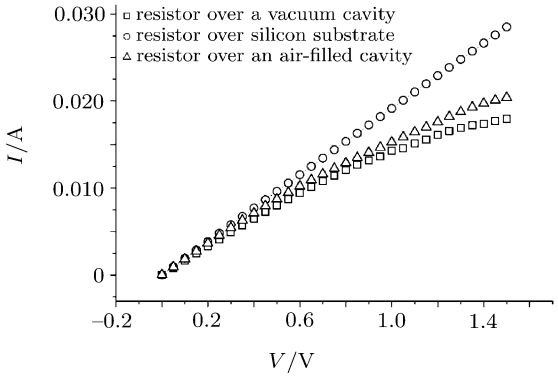


Fig.7. $I-V$ characteristics of three resistors in Fig.6.

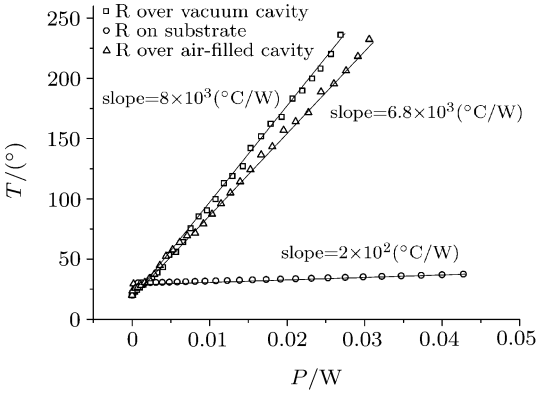


Fig.9. Calculated result of resistor temperature vs power inputs.

4.3. Frequency response

Because appropriate velocity fluctuations are not available for our test, we relies on electronic test signals to measure the time constant.[12] According to both theoretical analyses[13] and experimental confirmation,[14] the frequency response or time constant can be obtained by feeding an electronic sine wave or square wave into

the constant-current (CC) circuit. We pass a square wave into the E_t terminal of CC circuits (Fig.10) and observe the change of the voltage across the resistor as a function of time (Fig.11).The measurement shows that the time constants are on the order of several hundred microseconds, and the cutoff frequency is about 2 kHz as showed in Fig.12.

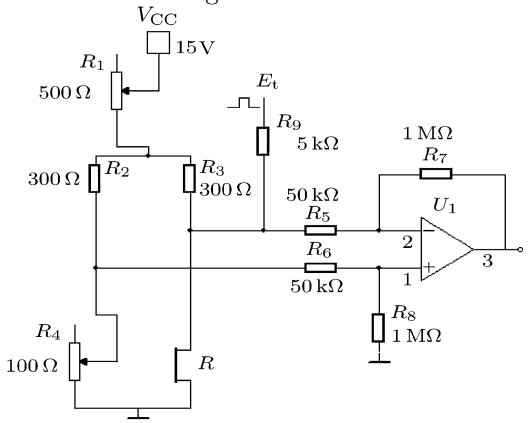


Fig.10. The circuit used for constant-current mode wind-tunnel measurements. R is the shear-stress sensor resistor.

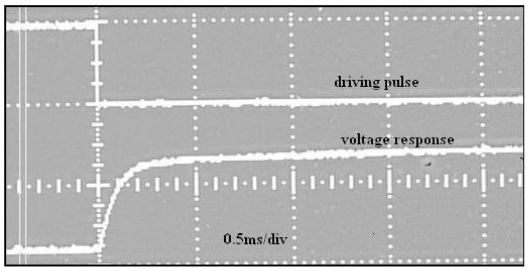


Fig.11. Voltage output for the time-constant measurement in still air.

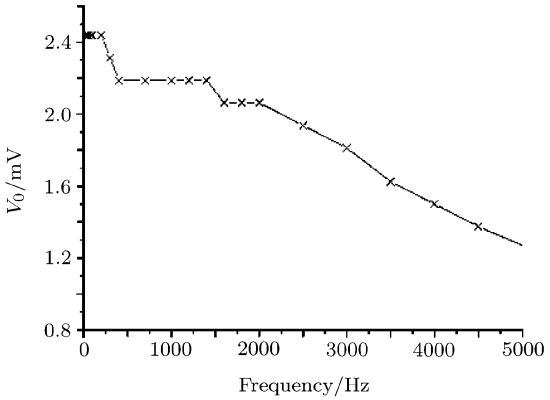


Fig.12. Frequency response curve of a typical sensor.

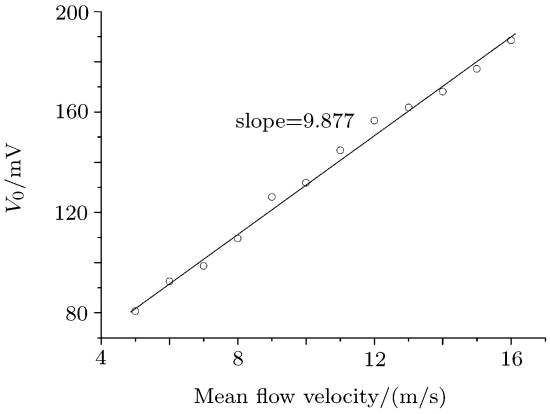


Fig.13. Output voltage as a function of the wind-tunnel mean-flow velocity for shear-stress sensors (constant current 20 mA).

4.4. Wind-tunnel tests

We use CC mode circuit for wind-tunnel tests of the micromachined shear-stress sensors. Figure 13 shows with the mean-stream velocity range from 5–16 m/s the output voltage as a function of the mean-flow velocity, and the slope of the response is 9.877 mv/(m/s).

5. Conclusions

A micromachined thermal shear-stress sensor with a cavity underneath has been developed. Comparing with the used sacrificial layer technique, we totally avoid the adhesion problem by using the vacuum anodic bonding and bulk-si anisotropic wet etching process to fabricate the sensor. This method, which makes the process very easy, not only avoids adhesion problem, but also does not influence the vacuum chamber's adiabatic effect. Thermal isolation experiment and wind tunnel tests show that the sensor with a cavity performed better than other sensors.

References

[1] Jiang F, Xu Y, Weng T X, Han Z G, Tai Y C, Huang A, Ho C M and Newbern S 2000 *IEEE Int. Conference on Micro Electro Mechanical Systems (MEMS)* pp364–369

[2] Jiang F, Tai Y C, Gupta B, Goodman R, Tung S, Huang J B and Ho C M 1996 *Proceedings of the IEEE International Conference on Micro Electro Mechanical Systems (MEMS)* pp110–115

[3] Xu Y, Jiang F, Newbern S, Huang A, Ho C M and Tai Y C 2003 *Sensors and Actuators* A **105** 321

[4] Haritonidis J H 1989 *Advances in Fluid Mechanics Mea-*

surements (Berlin: Springer) pp229–261

[5] Goldstein R J 1983 *Fluid Mechanics Measurements* (Taylor & Francis) p61

[6] Huang J B, Ho C H, Tung S, Liu C and Tai Y C 1995 *Instrumentation and Measurement Technology Conference IEEE* **24–26** 171

[7] Liu C, Huang J B,Zhu Z J, Jiang F,Tung S, Tai Y C and Ho C M 1999 *Journal of Microelectromechanical System* **8** 90

[8] Li R J and Li C B 2002 *Acta Phys. Sin.* **51** 1743 (in Chinese)

[9] Hanratty T J and Cambell J A 1983 *Fluid Mechanics Measurements* (New York: Hemisphere) pp559–615

[10] Saran A, Abeysinghe D C, Deshmukh P J, Flenniken R and Boyd J T 2003 *The 12th International Conference on Solid Stale Sensors, Actuators and Microsystem* pp564–567

[11] Kovacs G T A and Zhang W D 2000 *Micromachined Transducers Sourcebook* (Beijing: Science) p86

[12] Huang J B, Liu C, Jiang F K, Tung S, Tai Y C and Ho C M 1995 *IEEE* 1995 *Region* 10 *Conf. Microelectronics and VLSI* 570

[13] Freymuth P 1977 *J. of Physics* E: *Scientific Instruments* **IO** 705

[14] Moen M J and Schneider S P 1993 *Thermal Anemometry* ed. D E Stock, S A Sherif, A J Smits and I Davidson (New York: ASME) pp249–261